All-optical parallel-to-serial conversion by holographic spatial-to-temporal frequency encoding

P. C. Sun, Y. T. Mazurenko,* W. S. C. Chang, P. K. L. Yu, and Y. Fainman

Department of Electrical and Computer Engineering, University of California, San Diego, La Jolla, California 92093-0407

Received April 4, 1995

Optical processors that perform parallel-to-serial and serial-to-parallel data conversion are introduced and experimentally demonstrated for long-distance optical communication networks. © 1995 Optical Society of America

The bandwidth and the efficiency of fiber-optic communication systems exceed those of electrical cable systems. However, currently we are far from realizing the potential performance of optical networks. Electronic devices and systems connected to optical networks may reach bit rates in the range of gigabits per second. In contrast, the maximum bit rate of a photonic network may exceed 1 Tbit/s, limited by the performance of the optical fiber. The 3-order-of-magnitude mismatch between fiber and device capacity can be exploited to increase the speed, security, and reliability in the data transmission. Several all-optical methods exploiting this bit-rate mismatch have been investigated for controlling data streams in communication channels so that this bandwidth can be used more efficiently.[1–8]

The principle of spectral holography has been used for optical pulse shaping.[1,2] The combination of spectral holography with conventional spatial Fourier-transform holography permits the conversions of temporal signals into spatial signals and vice versa.[3–5] Dynamic spectral holography or spectral nonlinear optics can realize these conversions in real time, thus providing the possibility for all-optical time-division multiplexing and demultiplexing of broadband data streams. Dynamic time-to-space conversions of ultrashort light pulses (all-optical serial-to-parallel conversion) based on this principle have been demonstrated with four-wave[4,5] and three-wave[6] interactions. In this Letter we analyze and experimentally demonstrate this principle with a holographic optical processor that permits parallel-to-serial (i.e., space-to-time) optical signal conversion. Moreover, by combining our technique with existing serial-to-parallel conversion methods[4,5] we demonstrate experimentally the possibility of transmitting parallel optical signals over long-distance optical fiber networks.

The all-optical parallel-to-serial conversion processor is shown schematically in Fig. 1(a). The processor consists of two independent optical channels for carrying temporal signals and spatial signals. The temporal information-carrying channel consists of a pair of gratings and a 4-F lens arrangement. The incident pulses are transformed by the input reflecting grating and the first lens into a temporal frequency spectrum distributed in space of the focal plane, while the second lens and the output reflecting grating are performing the inverse transformation of the temporal spectrum distribution back to the time domain. The spatial information-carrying channel utilized with a cw laser source is a simple optical spatial Fourier-transform arrangement consisting of the input image and the reference waves introduced via a beam splitter to share the second lens of the temporal channel in the backward direction. To achieve interaction between the temporal and spatial frequencies information we use a real-time holographic material in a four-wave mixing arrangement. In this Letter we provide theoretical and experimental results that demonstrate all-optical parallel-to-serial conversion of a one-dimensional (1-D) spatial signal.

Let a spatially collimated and temporally transform-limited optical pulse propagating in the z' direction (see Fig. 2) be described by

$$s(t) = p(t - t_0)\exp(j\omega_c t), \tag{1}$$

where $p(t)$ is the temporal envelope function of the pulse, t_0 is the initial time, and ω_c is the carrier frequency. In the frequency domain, each frequency component of the pulse is described by

$$S(\omega) = P(\omega - \omega_c)\exp[-j(\omega - \omega_c)t_0], \tag{2}$$

where $P(\omega)$ is the temporal Fourier transform of the function $p(t)$. Assuming that the system of Fig. 2 is

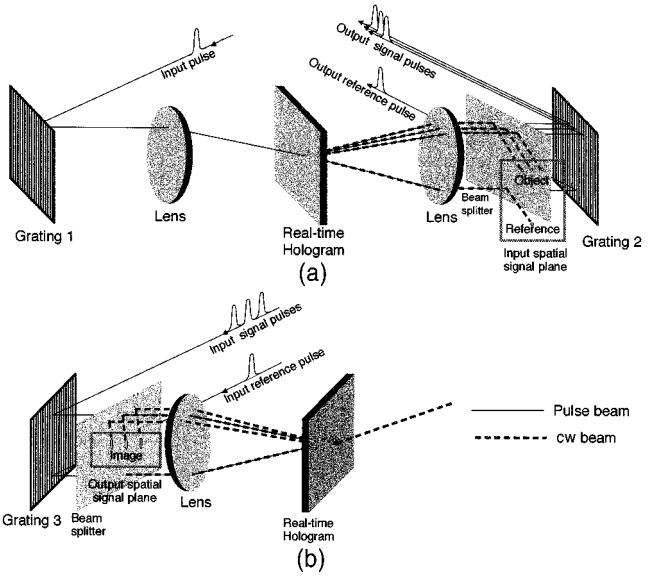

Fig. 1. Schematic diagram of optical processors for (a) parallel-to-serial and (b) serial-to-parallel conversions.

0146-9592/95/161728-03$6.00/0

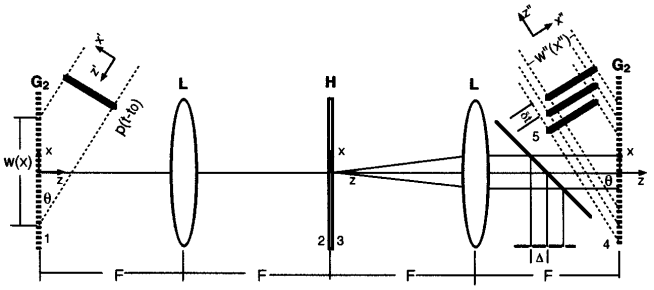

Fig. 2. Schematic diagram of parallel-to-serial conversion with four-wave mixing in real-time holograms: L's, lenses; H, hologram.

linear and time invariant, the output of the system is determined by the convolution of the input pulse with the system impulse response (or, equivalently, by the inverse Fourier transformation of the product between the spectrum of the input pulse with the system temporal transfer function). In the following we derive the temporal transfer function of the system using conventional Fourier optics analysis.

Consider a monochromatic plane wave of frequency ω incident upon the first reflecting grating at an inclination angle θ. The grating is arranged to diffract the carrier frequency component ω_c into the direction of the optical axis of the system. Thus the diffracted optical field of frequency ω in plane 1 is given by

$$s_1(x;\,\omega) = \exp\left[-j\,\frac{(\omega-\omega_c)}{c}\,\alpha x\right] w(x), \tag{3}$$

where $\alpha = \sin\theta$ and $w(x)$ is the pupil function of the reflecting grating. The field in plane 2 is determined by the spatial Fourier transform of the field in plane 1, yielding

$$s_2(f_x;\,\omega) = W\left[f_x + \frac{(\omega-\omega_c)}{2\pi c}\,\alpha\right], \tag{4}$$

where $W(f_x)$ is the spatial Fourier transform of $w(x)$, $f_x = \omega x/2\pi cF$, and F is the focal length of the lens. Equation (4) shows that if an input optical pulse is introduced into the system it will be spatially dispersed in the Fourier-transform plane, where each spectral component occupies a width determined by the function $W(f_x)$. Let a spatial Fourier-transform hologram in Fig. 2 be recorded by the spatial Fourier-transform setup shown in Fig. 1(a). The hologram contains information on the spatial Fourier transform of a sequence of equally spaced coherent point sources in which each corresponds to a single bit of data from a spatially distributed data array. The hologram serves as a temporal frequency filter with transmittance

$$t(f_x) = \sum_n A_n \exp\left[j2\pi n\Delta\left(\frac{\omega_w}{\omega} f_x\right)\right], \tag{5}$$

where A_n is the amplitude of the nth bit in the spatial data array, Δ is the spatial separation between adjacent elements in the data array, ω_w is the optical frequency of the writing field used for recording the hologram, and the spatial carrier frequency term has been neglected. The ratio ω_w/ω accounts for the difference in spatial frequencies of the spatial and temporal optical channels. Thus the field behind the hologram in plane 3 is $s_3(f_x;\,\omega) = s_2(f_x;\,\omega)t(f_x)$, with $s_2(f_x;\,\omega)$ and $t(f_x)$ from Eqs. (4) and (5), respectively.

The second spatial Fourier transform yields the optical field in plane 4:

$$s_4(x;\,\omega) = \sum_n A_n w\left[-x + n\left(\frac{\omega_w}{\omega}\,\Delta\right)\right] \times \exp\left\{\left(j\,\frac{(\omega-\omega_c)}{c}\,\alpha\left[x - n\left(\frac{\omega_w}{\omega}\,\Delta\right)\right]\right\}, \tag{6}$$

where the minus in $w(-x)$ indicates that the image is inverted. The field in plane 4 is diffracted by the second reflecting grating, yielding the output field propagating in the z'' direction:

$$s_5(x'';\,\omega) = \sum_n A_n w''\left[-x'' + n\left(\frac{\omega_w}{\omega}\,\Delta\right)\alpha\right] \times \exp\left[-j\,\frac{n(\omega-\omega_c)\omega_w\Delta}{c\omega}\,\alpha\right], \tag{7}$$

where a coordinate rotation from (x, z) to (x'', z'') is performed. Equation (7) represents the temporal transfer function of the system.

Finally, when a short optical pulse is introduced to the input, the system output is determined by the inverse Fourier transform of the product of Eqs. (2) and (7):

$$s_0(x'';\,t) = F_\omega^{-1}\{P(\omega-\omega_c)\exp[-j(\omega-\omega_c)t_0]s_5(x'';\,\omega)\}. \tag{8}$$

The function $P(\omega-\omega_c)$ is band limited with a bandwidth of $\Delta\omega$. If this bandwidth is much smaller than the central frequency ω_c (for our case, the pulse of ~150 fs with a central wavelength at 480 nm has a $\Delta\omega/\omega_c$ of ~1%), then the ω_w/ω values in Eq. (7) can be approximated by ω_w/ω_c and Eq. (8) can be solved as

$$s_0(x'';\,t) = \left[\sum_n A_n w''(-x'' + n\Delta'')p(t - t_0' - n\delta t)\right] \times \exp(+j\omega_c t), \tag{9}$$

where $\Delta'' = \alpha\omega_w\Delta/\omega_c$, $\delta t = \alpha(\omega_w\Delta/\omega_c c)$, and t' denotes the time delay in the system. Equation (9) shows a temporal sequence constructed of original incident pulses. The pulses are separated from one another by the same distance δt and are modulated in amplitude with a one-to-one correspondence to the data array from the spatial channel. Therefore, information is converted from space (parallel) to time (sequence) through the interaction of the corresponding frequency components. Note that the output pulses obtained with this technique propagate in the same direction but with slightly different transverse extents as a result of the difference in projections of the entrance pupil $w(x)$ on the output grating. This may cause a slight variation in coupling efficiency when these pulses are coupled into an optical fiber.

The parallel-to-serial conversion experiments were implemented with the processor shown in Fig. 1(a) (transmitter node) with the 1-D binary data array of Fig. 3(a). The output pulses [Fig. 3(b)] were transmitted to the input of the processor shown in Fig. 1(b)

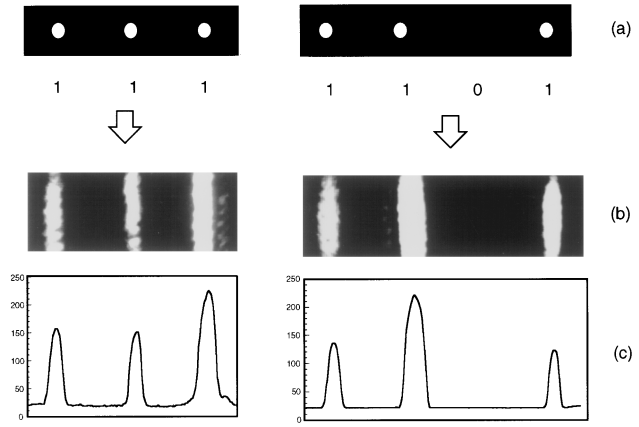

Fig. 3. Experimental results of image transmission with parallel-to-serial and serial-to-parallel conversion: (a) photograph of the 1-D input data arrays, (b) photograph of the 1-D binary data array images reconstructed at the receiver, (c) plots of the intensity distributions in (b).

(receiver node) that implements serial-to-parallel conversion [Figs. 3(b) and 3(c)]. A single reference pulse produced by the nondiffracted portion of the readout beam in Fig. 1(a) was also transmitted to the receiver for decoding. The serial-to-parallel conversion[4,5] is based on the recording of a spectral hologram between the input signal pulses and the reference pulse [Fig. 1(b)]. The cw monochromatic readout wave is diffracted and modulated by the spatial frequencies of the spectral hologram and Fourier transformed by a lens [Fig. 1(b)]. The reconstructed one-dimensional spatial image shown in Fig. 3(b) exhibits one-to-one correspondence with the transmitted image of Fig. 3(a).

We performed the experiments using 150-fs optical pulses of 1-kW peak power at a wavelength of 480 nm generated from a frequency-doubled mode-locked Ti:sapphire laser. The spatial Fourier-transform hologram of the 1-D binary data array shown in Fig. 3(a) was recorded in a 1-mm-thick photorefractive crystal of lithium niobate with the 488-nm line of an Ar^+ laser. A small angle between the reference and the object beams was used to ease the Bragg-matching requirement for the reconstruction with the optical pulse at a center wavelength of 480 nm. The resultant output pulses and the reference pulse were transmitted to the receiver by free-space propagation. In practice, the signal and the reference pulses can be transmitted through two identical fiber or through a single fiber by polarization multiplexing. In our experiments the output pulses and the reference pulse were transmitted through a low-pass spatial filter to emulate the transmission through a fiber, i.e., to ensure that there is no spatial information transmitted to the receiver. At the receiver we recorded a spectral hologram between the input signal pulses and the reference pulse, using another photorefractive lithium niobate crystal. The spectral hologram was read out with the 488-nm line of an Ar^+ laser and then Fourier transformed by a lens to yield the serial-to-parallel converted 1-D spatial output signal shown in Fig. 3(b). The resultant images are stretched in the vertical direction because of the nature of the spectral holograms, which are inherently 1-D. Note that the speed of transformations in our experiments was limited by the time response of the photorefractive lithium niobate crystal (~ 5 s). In the future we are planning to use fast nonlinear optical materials such as photorefractive semiconductor crystals and semiconductor microstructures to provide high-speed operation.

If the input pulse has a wide bandwidth, Eq. (9) becomes invalid because higher-order terms from the Taylor expansion of $(\omega - \omega_c)/\omega$ need to be taken into consideration, which will result in dispersed signal pulses. The dispersion reflects the frequency mismatches between the spatial channel and the temporal channel and will appear in the signal pulses but not in the reference pulse. Information on these frequency mismatches will be carried to the receiver node to be transformed onto the spectral hologram. Therefore the spectral hologram at the receiver would resemble the original spatial Fourier-transform hologram at the transmitter. This phenomenon in spectral holography can be seen as temporal phase conjugation. The demonstrated parallel-to-serial and serial-to-parallel conversions by holographic processors possess additional advantages: (1) they do not require transform-limited input pulses, since the system is self-referenced, and (2) optical dispersion induced by the holographic materials, the communication channel, and all-optical components is self-compensated, because the reference beam propagates through the same material as the signal beam.

In conclusion, we have introduced and experimentally demonstrated optical processors that perform parallel-to-serial and serial-to-parallel data conversion for transmission of 1-D images and image-format data. This approach is suitable for long-distance communication of parallel information through all-optical fiber networks.

This research was supported in part by National Science Foundation grants ECS-9311062 and ECS-9415834, Advanced Research Projects Agency grant OTCII-MDA 972-94-1-002, and NATO grant HTECH.CRG 931141. Y. T. Mazurenko thanks the Russian Foundation for Fundamental Research (project code 93-02-14826) for supporting his research.

*Permanent address, S. I. Vavilov State Optical Institute, 199034, St. Petersburg, Russia.

References

1. Y. T. Mazurenko, Appl. Phys. B **50,** 101 (1990).
2. A. M. Weiner, D. E. Leaird, D. H. Reitze, and E. G. Paek, IEEE J. Quantum Electron. **28,** 2251 (1992).
3. Y. T. Mazurenko, Opt. Spectrosc. **57,** 1 (1984).
4. K. Ema, M. Kuwata-Gonokami, and F. Shimizu, Appl. Phys. Lett. **59,** 2799 (1990).
5. M. C. Nuss, M. Li, T. H. Chiu, A. M. Weiner, and A. Partovi, Opt. Lett. **19,** 664 (1994).
6. Y. T. Mazurenko, A. S. Spiro, S. E. Putilin, and A. G. Beliaev, Opt. Spectrosc. **78,** 122 (1995).
7. M. B. Danailov, I. P. Christov, and N. I. Michailov, Appl. Phys. B **49,** 371 (1989).
8. K. G. Purchase, D. J. Brady, and K. Wagner, Opt. Lett. **18,** 2129 (1993).